AD-A034 950 NAVAL RESEARCH LAB WASHINGTON D C F/G 20/5
HEAT CONDUCTION IN THREE DIMENSIONS.(U)
DEC 76 S T HANLEY
UNCLASSIFIED NRL-8066 NL

1 OF 1
AD A034950

END

DATE
FILMED
3 - 77

NRL Report 8066

Heat Conduction in Three Dimensions

S. T. HANLEY

High Energy Laser Facility
Optical Sciences Division

December 6, 1976

NAVAL RESEARCH LABORATORY
Washington, D.C.

SECURITY CLASSIFICATION OF THIS PAGE (When Data Entered)

REPORT DOCUMENTATION PAGE

READ INSTRUCTIONS BEFORE COMPLETING FORM

1. REPORT NUMBER: NRL Report 8066	2. GOVT ACCESSION NO. / 3. RECIPIENT'S CATALOG NUMBER
4. TITLE (and Subtitle): HEAT CONDUCTION IN THREE DIMENSIONS	5. TYPE OF REPORT & PERIOD COVERED: Interim report on a continuing NRL problem.
	6. PERFORMING ORG. REPORT NUMBER
7. AUTHOR(s): S.T. Hanley	8. CONTRACT OR GRANT NUMBER(s)
9. PERFORMING ORGANIZATION NAME AND ADDRESS: Naval Research Laboratory, Washington, D.C. 20375	10. PROGRAM ELEMENT, PROJECT, TASK AREA & WORK UNIT NUMBERS: NRL Problem R05-31D, Project 0RD-017/173-1U1754
11. CONTROLLING OFFICE NAME AND ADDRESS: Department of the Navy, Naval Sea Systems Command (PM-22/PMS-405), Washington, D.C. 20362	12. REPORT DATE: December 6, 1976
	13. NUMBER OF PAGES: 26
14. MONITORING AGENCY NAME & ADDRESS (if different from Controlling Office): 12 26p.	15. SECURITY CLASS. (of this report): Unclassified
	15a. DECLASSIFICATION/DOWNGRADING SCHEDULE

16. DISTRIBUTION STATEMENT (of this Report) 16 U1754

Approved for public release; distribution unlimited.

17. DISTRIBUTION STATEMENT (of the abstract entered in Block 20, if different from Report)

18. SUPPLEMENTARY NOTES

19. KEY WORDS (Continue on reverse side if necessary and identify by block number)

Diffusion processes
Finite difference methods
Heat conduction
Laser heating
Thermal damage
Thermal load

20. ABSTRACT (Continue on reverse side if necessary and identify by block number)

An applications-oriented numerical solution to the heat diffusion equation in three dimensions, with local temperature dependence in the thermal parameters and including phase changes, has been developed. Comparisons with exact one-dimensional solutions and experimental data indicate better than 10% accuracy in predicting internal slab temperatures. Rapid thermalization of water-cooled mirrors under high power densities is predicted. Possible applications to work in thermal signatures of irradiated targets are suggested.

DD FORM 1 JAN 73 1473 EDITION OF 1 NOV 65 IS OBSOLETE
S/N 0102-014-6601

SECURITY CLASSIFICATION OF THIS PAGE (When Data Entered)

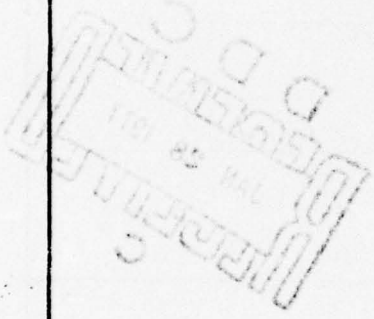

CONTENTS

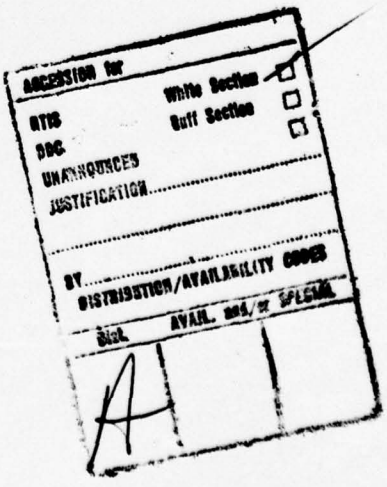

HEAT CONDUCTION IN THREE DIMENSIONS

INTRODUCTION

There is a need for accurate three-dimensional heat transport prediction in many areas of applied research, including solidification of molten materials, ablation of missile skins under aerodynamic heating, vulnerability of targets under thermal loads, and characterization of high-power mirror surfaces under extreme thermal loads. In some cases the problem can adequately be described by unidimensional heat flux, but many problems cannot be solved in a convenient and general form without the added dimensions of transverse heat flow. The ongoing laser damage and vulnerability program in the Department of Defense could more effectively make use of limited test schedules with the aid of a three-dimensional code combining accuracy and computational ease. Despite the importance of the topic, the literature reveals few solutions that may be extended to practical problems of the type proposed here.

In an effort to satisfy this need, and in particular to characterize some high-power water-cooled mirrors for future use at the Optical Radiation Laboratory at Chesapeake Beach, Md., a standard finite-difference approximation has been initiated to solve the three-dimensional heat diffusion equation

$$\frac{\partial T}{\partial t}(x, y, z, t) = \alpha \nabla^2 T(x, y, z, t). \tag{1}$$

The complete difference form of this equation is used to provide maximum execution speed for a modest lattice point density. Although there are more elaborate digital techniques which would afford improved accuracy with the same lattice density, the additional program complexity does not justify the slight increase in accuracy near the fusion front (see for example Murray and Landis [1]).

Comparisons have been made in the limiting case of a "flood-loaded" sample with unidirectional heat flow to an exact premelting solution for temperature rise in a semi-infinite slab in one dimension and to internal temperature profiles derived from a highly refined fifty-subdivision one-dimensional finite-difference code by S.T. Hanley [2]. The agreement is better than 10% both in internal temperature profile and in burn-through prediction.

FINITE-DIFFERENCE MODEL

The material to be heated or cooled is modeled to a rectangular slab with arbitrary length, width, and thickness and with the thermal load applied to the front surface. Before heat can diffuse into the interior of the slab, a thermal "step" must take place at the front surface; this is described by the basic heat conduction equation,

$$-K\overline{\nabla T} = P_0 A \tag{2}$$

Manuscript submitted September 9, 1976.

in which P_0 is the incident heat flux and A is the absorption coefficient or fraction of incident power density coupled into the material. K is the thermal conductivity for the material and is treated as a temperature-dependent parameter. The finite-difference approximation used for this equation is given in the forward difference form by

$$T(i, j, k, \ell+1) = T(i, j, k, \ell) + \frac{P_0}{K} A\cos\theta\,\Delta Z \tag{3}$$

where a cosine function has been introduced to allow arbitrary incidence angles θ from normal to the front surface. The X-Y plane is chosen to be the front surface, with the origin at one corner. The subscripts i, j, and k refer to lattice points along the X, Y, and Z axes, and ℓ refers to integral multiples of the step Δt along the time axis. At present no loss terms are explicitly included for heat carried away by convective cooling or radiation from the front surface. Under many applications these terms represent a negligible fraction of the heat input (< 30 W/cm^2 for front surface temperatures less than 2000K). Loss terms of this type are implicitly treated in temperature-dependent absorption coefficient A, which also accounts for changes in surface reflectivity.

The complete difference approximation for the diffusion of heat into the interior of the slab in given by

$$\begin{aligned} T(i, j, k, \ell+1) = T(i, j, k, \ell) &+ \frac{\alpha\Delta t}{\Delta X^2}\,[T(i+1, j, k, \ell) + T(i-1, j, k, \ell)] \\ &+ \frac{\alpha\Delta t}{\nabla Y^2}\,[T(i, j+1, k, \ell) + T(i, j-1, k, \ell)] \\ &+ \frac{\alpha\Delta t}{\Delta Z^2}\,[T(i, j, k+1, \ell) + T(i, j, k-1, \ell)] \\ &- 2\alpha\Delta t\left(\frac{1}{\Delta X^2} + \frac{1}{\Delta Y^2} + \frac{1}{\Delta Z^2}\right) T(i, j, k, \ell). \end{aligned} \tag{4}$$

The usual simplification of choosing Δt such that the $T(i, j, k, \ell)$ term vanishes cannot be made because of the temperature dependence of the diffusivity

$$\alpha(T) = \frac{K(T)}{C(T)\rho\,(T)}, \tag{5}$$

where ρ and C are the density and specific heat, respectively. The code does select a time step Δt as a function of ΔX, ΔY, ΔZ, and the materials thermal parameters which will provide a stable convergent solution. Stability is taken in the sense that short-wave disturbances are damped out. A slight improvement in accuracy in the internal approximate solution to the diffusion equation was obtained by going to smaller time steps than that required for stability, with the lattice density remaining fixed in a manner analogous to the one-dimensional example given by Özisik [3]

The edge and back surfaces are independently constrained to satisfy one of two boundary conditions. The first is that of no heat flow across the boundary, resulting in

$$-K \nabla T = 0 \tag{6}$$

for all lattice points on that surface. A simple forward difference approximation to the gradient is used here, as in Eq. (3). The alternative boundary condition is to heat sink all lattice points in that surface to the ambient or initial slab temperature.

At the instant any lattice point reaches the melting temperature for the material, an additional boundary condition is applied:

$$\frac{\partial m}{\partial t} = \frac{K}{L} \sum_n \overline{\nabla}_n T_s - \frac{K}{L} \sum_n \overline{\nabla}_n T_\ell \tag{7}$$

where L is the latent heat of fusion for the material. This equation is used to follow the position of the liquid-solid interface along the permissible axis directions $\pm i$, $\pm j$, and $\pm k$. Once a lattice point reaches the melt temperature it is pinned at the melt temperature until the heat flow into the unit cell about the lattice point minus the heat flow out, as evaluated with Eq. (7) along the six unit vector directions, is equal to the latent heat of melting for the mass of the unit cell. After this balance has been met, the lattice point temperature is allowed to rise. In this manner the melt surface progresses through the interior of the slab as dictated by the local thermal gradients. This model is quite powerful in dealing with irregular thermal load profiles on the front surface. Care must be taken to ensure that the time steps are small compared with the time required to melt a unit cell, in order to avoid excessive errors in fusion front travel. For the thermal loads considered here, this consideration is taken care of by the internal time step selection for stability.

A brief description of some of the program features will be given here, and a more detailed discussion of program construction and performance is given in Appendix A. The program has an internal library of materials containing thermal parameters with temperature dependence and is expandable to any material for which the constants are known. The lattice is made up of 10 equally spaced points per axis along the x and y axes and 11 equally spaced points along the z axis, providing an accuracy of better than 10% (as will be shown in the next section). The front surface thermal load is broken into three selectable categories. A "top hat" or uniform intensity distribution of arbitrary diameter and total power allows simulation of saturated laser amplifier configurations. A Gaussian distribution truncated at an arbitrary radius for the $1/e^2$ intensity allows modeling of laser TEM_{oo} beam profiles. The third distribution allows the user to specify point by point an arbitrary thermal load application. This flexibility of input distribution allows modeling of a wide variety of problems with a minimum of setup time.

APPLICATIONS

One of the first uses of the code was to scale high-reflectance water-cooled molybdenum mirrors with thermal load. An example of the predicted results is shown in Fig. 1. In the model, a truncated Gaussian beam of 4-cm radius impinges on a molybdenum slab of 0.05-cm

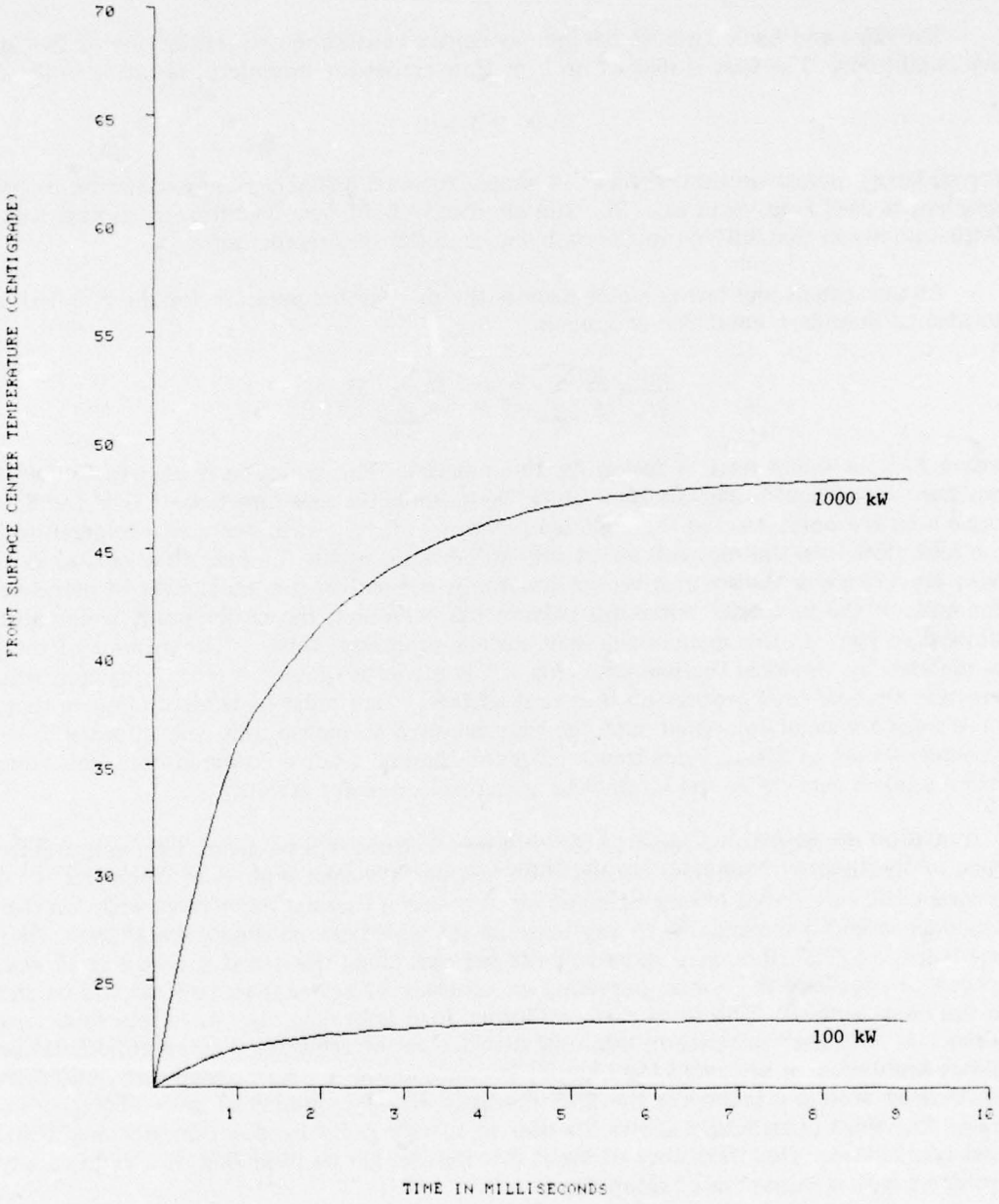

Fig. 1 — Thermal response of water-cooled molybdenum mirror. The front surface thermal response vs time is shown for a 98% reflective water-cooled molybdenum mirror at two power levels. The thermal load is produced by an 8-cm-diam Gaussian beam truncated at the $1/e^2$ intensity radius and having 100-kW and 1000-kW total power to produce the upper and lower curves, respectively. Faceplate thickness is 0.05 cm.

thickness with the back surface and edges heat sinked to ambient temperature. The front surface reflectivity is set at a fixed 98% to allow for aging and accumulation of impurities. Although enhanced silver coatings are better than this [4], it is difficult to maintain higher reflectance than this over a period of time. Two power levels are shown; the lower one represents nominal power densities commonly in use on high-power water-cooled mirrors, and the upper curve represents an extrapolation to potentially attainable power densities. The cooling passages in the mirror wall allow some water temperature rise due to the finite flow rate through the mirror. At the higher power level, the water temperature rise from inlet to outlet may reach 10°C. This effect has not been included in the model, however, since it depends on the design of flow passages. The 0.05-cm face plate thickness represents that found in some of the better chemically etched mirrors on the market today. The time required to reach stable thermal conditions is short at both power levels. Figure 2 shows an overhead view of the molybdenum slab of Fig. 1, with the temperature axis normal to the front surface. The incident beam power differs slightly from 1000 kW due to the finite number of lattice sites within the beam diameter. Internal program algorithms were designed to preserve flux densities specified by total power and beam diameter and then print out the quantized beam power, rather than scale flux density to total power.

A check of premelting accuracy was made by flood loading a slab of aluminum with a uniform beam distribution for times shorter than that required for heat diffusion to the back surface and comparing the internal temperature profile to the exact one-dimensional analytical result

$$T(z, t) = T_0 + 2AP_0 \left[\sqrt{\frac{t}{\pi K \rho C}} \exp\left(\frac{-Z^2 \rho C}{4Kt}\right) - \frac{z}{2K} \operatorname{erfc}\left(\frac{z}{2} \sqrt{\frac{\rho C}{Kt}}\right)\right] \tag{8}$$

for a semi-infinte slab of polished aluminum. The results after 0.05, 0.1, 0.15, and 0.2 s of irradiation are shown in Fig. 3. For purposes of comparison the temperature dependence of the thermal parameters in the three-dimensional code was suppressed. The upper curve of each pair is the three-dimensional finite-difference approximation to the exact one-dimensional analytical solution given in the lower curve. For all depths into the slab the accuracy is better than 10%. Several alternatives for improving accuracy are discussed in the subsequent section.

A limitation of thermal profiling models in the literature that claims high accuracy, such as the one-dimensional model of Fuhs and Fuhs [5], is the assumption of constant thermal parameters. To show the nature of this restriction, we irradiated a slab of polished aluminum with 20,000 W/cm^2 for 0.3 and 1.5 s. First with the temperature dependence contained in the thermal parameters and then with thermal dependence suppressed. The upper curve of each pair in Fig. 4 shows the error encountered by neglecting the temperature dependence. As might be expected, the error grows with increasing temperature and becomes appreciable after a modest amount of heating. In work on laser damage of materials such as the AVCO Everett study [6] done for the Air Force Materials Laboratory, significant improvement in modeling of experimental data should be obtained by including the effects of nonconstant specific heat, thermal conductivity, density, and absorption.

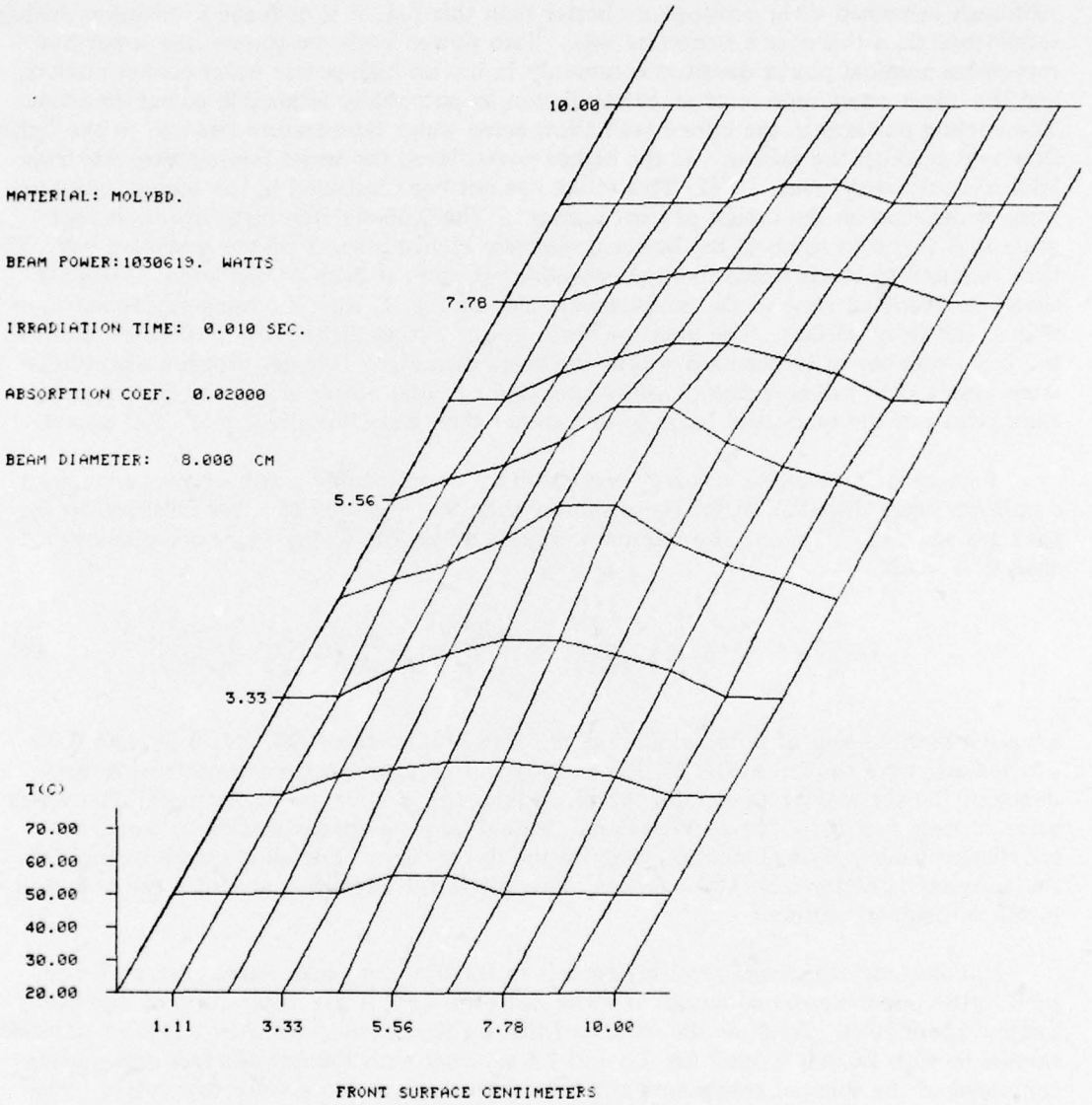

Fig. 2 — Surface plot of water-cooled molybdenum mirror under thermal load. Front surface temperatures. for a water-cooled molybdenum mirror under the conditions of Fig. 1 and at the 1000-kW power level. Shown after 10 ms of radition.

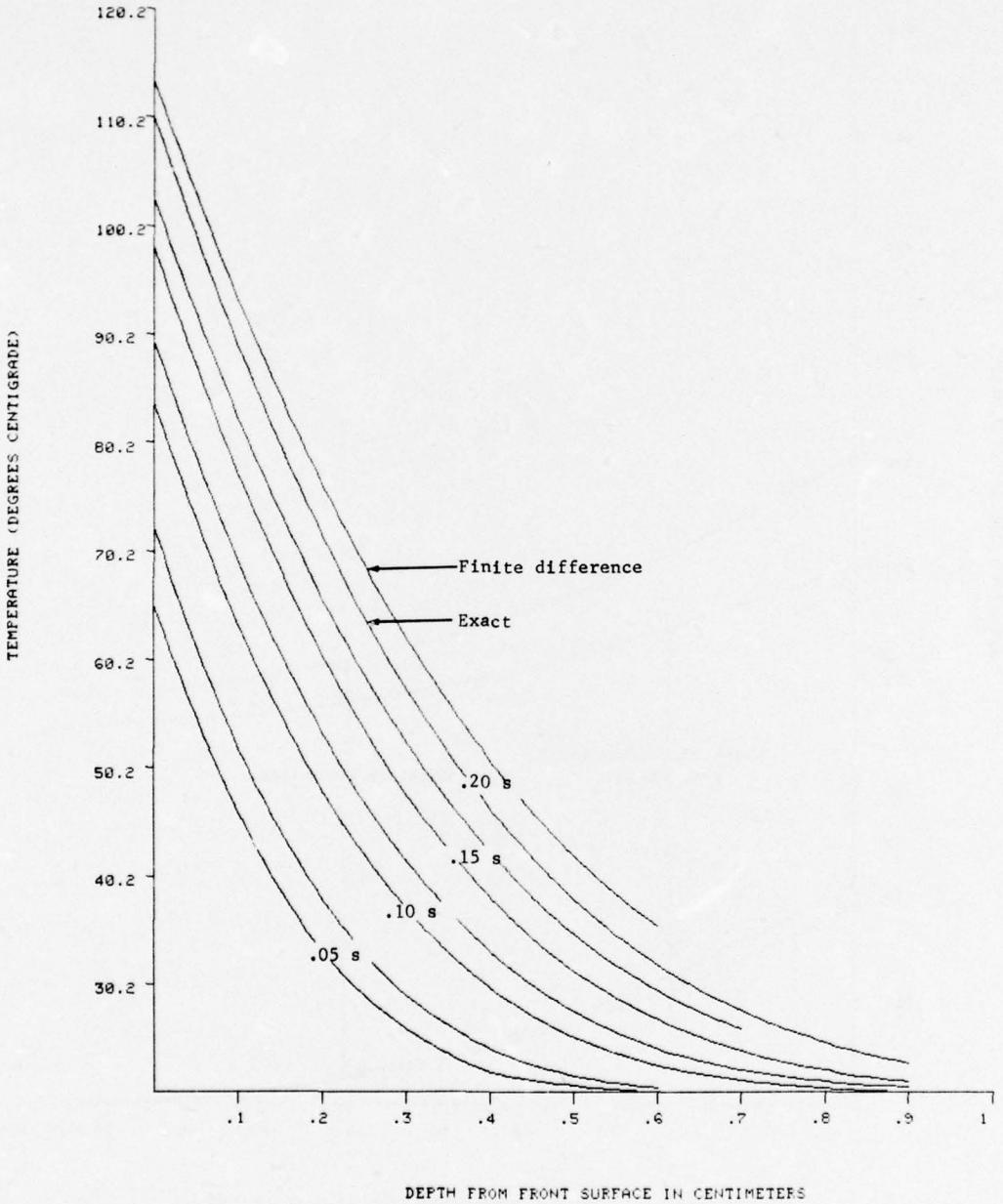

Fig. 3 — Comparison of three-dimensional code and one-dimensional analytical solution. The upper curve of each pair gives internal temperatures for a 1-cm-thick slab of aluminum 2024 uniformly flood loaded at 20000 W/cm^2 incident flux after 0.05, 0.1, 0.15, and 0.2 s of irradiation. Temperature dependence in all thermal parameters of the three-dimensional code are suppressed. The lower curve of each pair represents the exact one-dimensional analytical premelting solution for the same power density and at the respective times of irradiation.

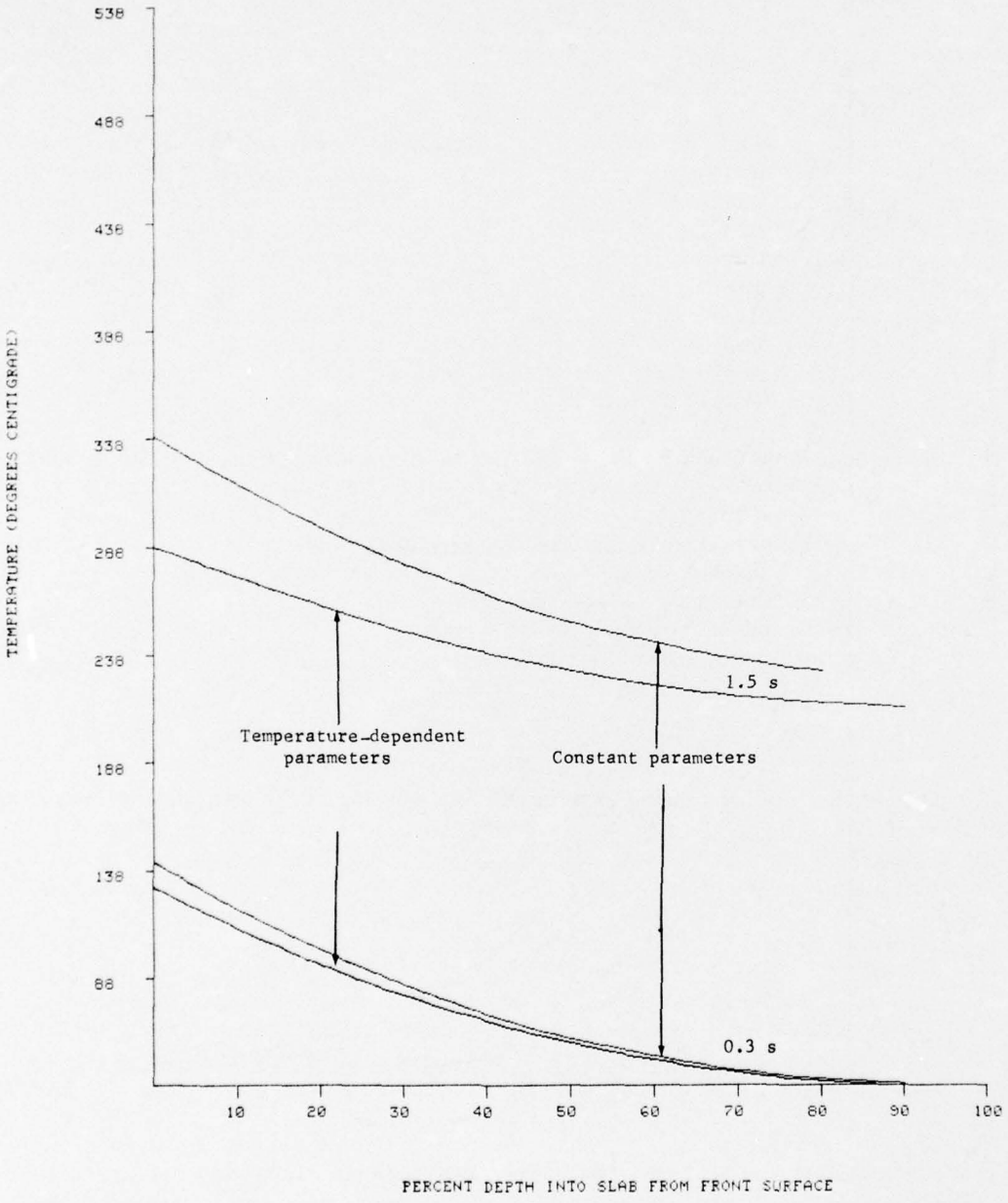

Fig. 4 — Temperature dependence in thermal parameters. Internal temperatures are shown for a 1-cm-thick slab of polished aluminum 2024 irradiated with 20000 W/cm^2 in a flood-loaded uniform distribution for 0.3 and 1.5 s. The temperature dependence of thermal parameters was suppressed in the upper curve of each pair to show the error introduced by neglecting temperature dependence.

Experimental measurements of burn-through times on aluminum panels painted with special "nonleafing" paint have been made by Dr. R. Wenzel of the Naval Research Laboratory (NRL). The samples were mounted vertically and irradiated at near normal incidence. Video coverage revealed retention of some liquid on the surface throughout the melting process. The measurements yielded a statistically averaged burn-through constant for given target thickness and irradiating peak power density. R.B. Brown, of NRL, performed absorption measurements on charred nonleafing paint samples and rough-melted aluminum samples at 10.6-μm wavelengths. To test all of the features of the three-dimensional code, we ran a simulation of the painted aluminum sample. Using for inputs to the three-dimensional temperature profiler Brown's measured absorption values for premelting and postmelting, temperature-dependent thermal parameters for aluminum 2024, a slab thickness and power density equal to that used by Wenzel in his measurements, and 45% of total slab thickness retained as liquid, we heated the sample from 20°C up to melting, and the melt interface progressed to the back surface within 5% of the average burn-through time measured by Wenzel.

As an additional check on the validity of the three-dimensional code for heating beyond the onset of melting, a comparison was made to the exact one-dimensional burn-through expression in the limiting ease of ablation (complete melt removal) and constant thermal parameters derived by J. Rogerson [7]. Burn through occurred in 5.78 s for a flood-loaded (beam diameter larger than sample) uniform beam of 20,000 kW/cm^2 incident on a polished aluminum 2024 slab 1 cm thick with 10% liquid layer retention (minimum layer of 3-D code at present) and with temperature dependence suppressed. This compared favorably with Rogersons exact value of 5.90 s under the same conditions.

DISCUSSION

One of the problems facing experimentalists working in the area of laser interactions with materials is the higher cost per shot and longer down time that are inherent in the trend toward large chemical lasers as compared with gas dynamic lasers. With the increased premium placed on experimental runs, the ability of this code to predict trends and aid selection of experiment parameters for maximum effectiveness of limited data becomes a valuable asset.

An area particularly well suited to modeling of the type discussed in this paper is in the development of hot spot tracking. With the addition of radiative and convective loss terms at the surface, modeling to thermal signatures from targets irradiated with arbitrary beam profiles could be performed using the existing three-dimensional code. By further modifying the code to exclude certain of the lattice points in the slab, geometries other than flat surfaces may be used for target simulation. The simulated thermal signature could be used to evaluate proposed hot spot tracking techniques and as an input toward improving working systems.

At present there are no solutions in the literature capable of predicting spatial distortions of optical surfaces under thermal loads, with the exception of simplified one-dimensional analyses such as that given by Fuhs and Fuhs [5]. The three-dimensional code presented here can in its present state give temperature-vs-time histories for arbitrary

thermal loading and boundary conditions, as shown in Figs. 1 and 2. With additions to the code, spatial distortion in the slab could be calculated directly from the slab temperature matrix at any given time. Such information could be used in all high-power optics configurations.

The error shown in Fig. 3, due to 10 subdivisions per axis and a standard finite-difference approach, can be reduced in several ways. The most straightforward would be to increase the lattice point density and thereby derive a better approximation to the derivatives in Eq. (1). This alternative also gives more surface lattice points with which to approximate beam profiles. On the other hand it would require more computation time and more memory space from the computer. A second alternative, which was demonstrated in one-dimension for finite-difference techniques by S.T. Hanley [2], is to expand the solution in spatial and time coordinates for improved accuracy with the same lattice density. There will be an increase in computation time with this alternative due to the increase in mathematical complexity. In the one-dimensional case mentioned above it was shown that comparable accuracy was achieved by either doubling the lattice density or using the coordinate expansion. As shown in Fig. 3, the nature of the error is a small offset or starting error in the time variable; the error remains essentially constant as heating progresses. An alternative procedure to increase accuracy would be to determine the offset as a function of lattice spacing, time step, and material parameters and start the time variable at a suitable positive offset value. To demonstrate the improvement in accuracy obtained by this last method, we determined the fixed time offset for the example used in Fig. 3; by starting the time variable at this positive value are obtained the agreement shown in Fig. 5. The accuracy is better than 2% throughout the depth of the slab and for all times greater than several offset steps.

A particular experimental problem in the laser heating of materials is measurement of the liquid layer retained on the front surface of the irradiated sample as burn-through progresses. This is difficult to measure directly and has a significant effect on burn-through times. Figure 6 shows back surface temperature rise vs time for a slab of aluminum 1 cm thick irradiated with a 44-kW Gaussian beam of 3-cm diameter and with 10%, 20%, 40%, 60%, and 100% liquid layers retained at the front surface as the melt progresses. The faster temperature rise corresponds with the thinner liquid layer retained. A measurement could be made with conventional back surface thermocouple techniques, and the melt layer could then be derived by comparison to a chart such as Fig. 6 for the slab under study.

ACKNOWLEDGMENTS

The author wishes to thank F.R. Fluhr, R.B. Brown, and Dr. R. Wenzel for valuable discussions and measurements.

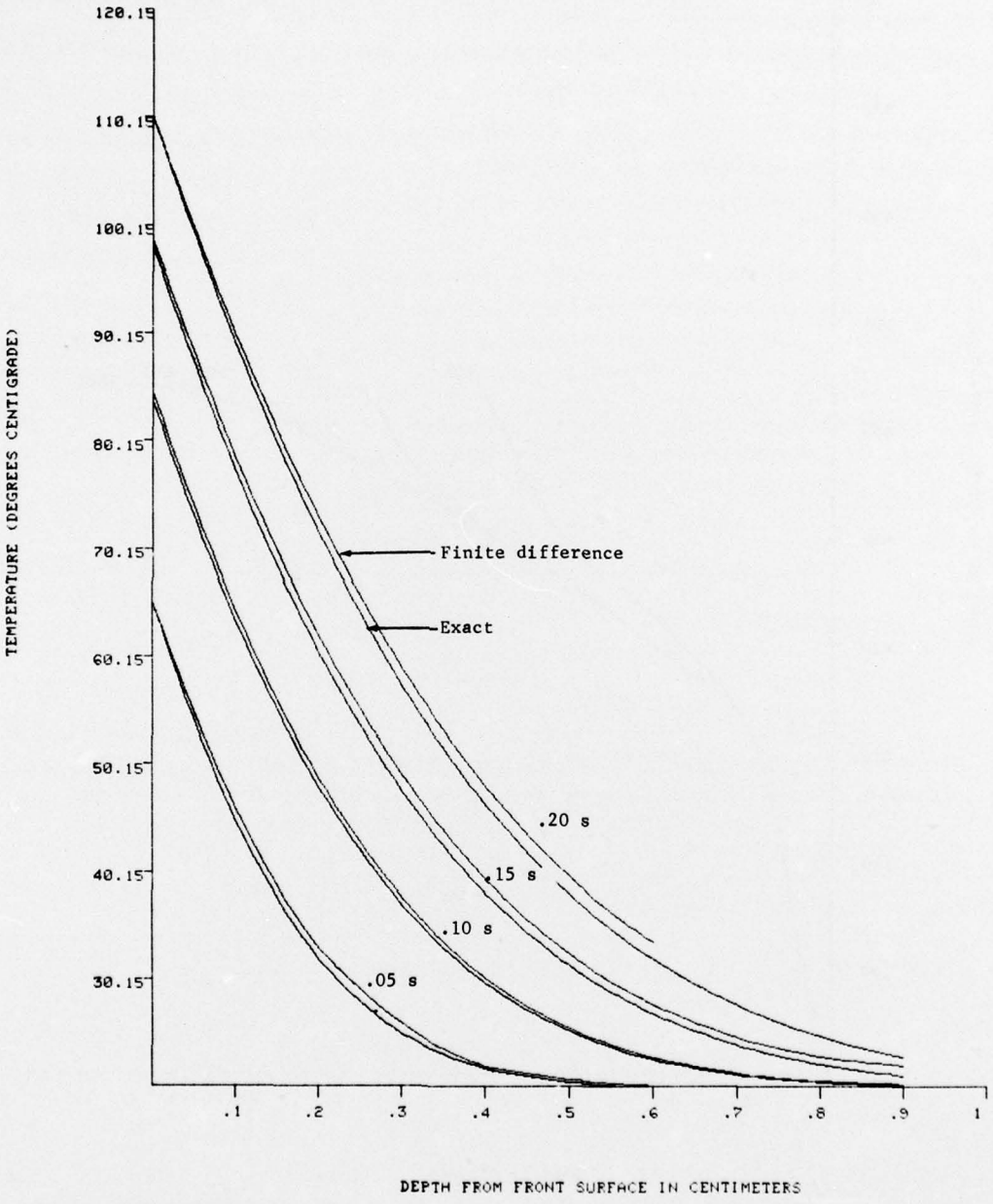

Fig. 5 — Improving accuracy by reducing starting error in time axis. Internal slab temperatures for aluminum 2024 under the conditions of Fig. 3 but with a time offset to reduce the starting error.

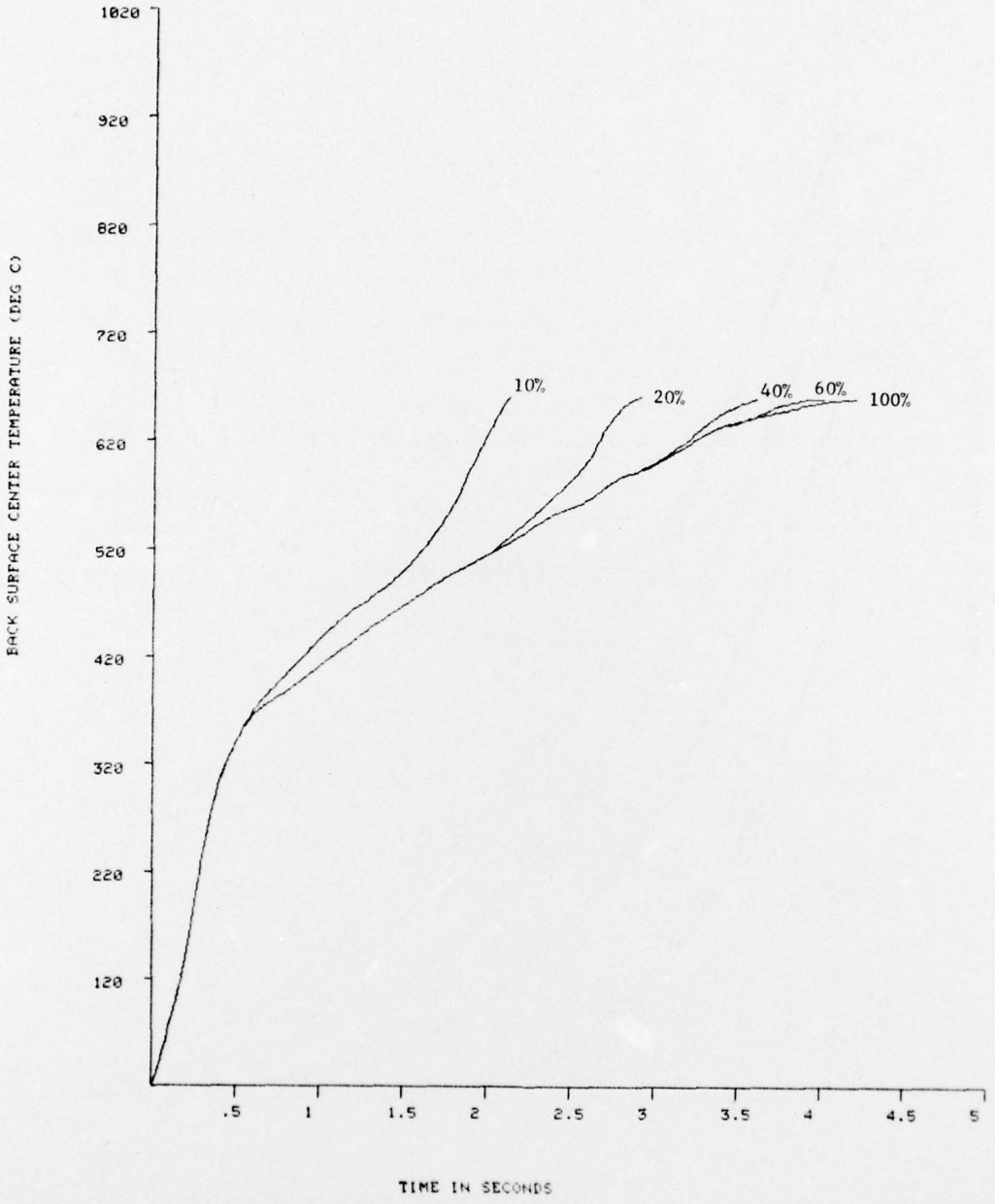

Fig. 6 — Back surface temperature signature vs melt removal. The center back surface temperature rise is given for a 1-cm-thick painted aluminum panel irradiated with a 3-cm truncated Gaussian beam of 44-kW total power at 10%, 20%, 40%, 60%, and 100% (of total slab thickness) liquid layer retention on front surface.

REFERENCES

1. W.D. Murray and F. Landis, "Numerical and Machine Solutions of Transient Heat Conduction Problems Involving Melting or Freezing," *Trans. ASME* 8 106-112 (1959).

2. S.T. Hanley, "A General Solution to the One- and Two-Dimensional Melting Using a Finite Difference Approach," NRL Report 7200, Nov. 1970.

3. M.N. Özisik, *Boundary Value Problems of Heat Conduction*, p. 396 International Textbook Co., Scranton, Pa., 1968.

4. Richard L. Pierce, "Metal Mirror Selection Guide," Spawr Optical Research Report 74-004, Sept. 1975.

5. A.E. Fuhs and S.E. Fuhs, "Computer-Drawn Graphs Help Calculate Effects of Heating by Laser Radiation," *Laser Focus*, 12 (No. 6), pp 66-73 (June 1976).

6. A. Mandl, "Aerodynamic Enhancement of Laser Damage to Titanium Alloys," Air Force Materials Lab. Technical Report 75-26, May 1975.

7. J.E. Rogerson and G.A. Chayt, "Total Melting Time in the Ablating Slab Problem," *J. Appl. Phys.* 42 (7) 2711-2713 (1971).

Appendix A

PROGRAM DESCRIPTION

The program is set up so that with an initial terminal question-and-answer period the user can select a material, an arbitrary slab geometry, an arbitrary beam profile, and an arbitrary run time. An internal library contains all the material parameters and allows the user simply to select a material without the aid of reference tables. The target thickness, length, and width are input in centimeters. Beam characteristics are input as total power in watts, diameter in centimeters, angle of incidence in degrees from normal, and selection of Gaussian, "top-hat", or user-specified experimental profile. The ambient or starting temperature is input in degrees centigrade, and boundary conditions of heat sinking to ambient or insulating among edges and back surface are selected. Output graphics are set up by inputting total run time and printout time interval for slab temperature arrays and plot and either front or rear surface to be plotted.

The programing is done in Fortran IV for improved computation speed over Basic. The ratio of run times for the two programing languages on the PDP-11 is approximately 40 for a program of this type. The entire program is core resident on a 28K-PDP 11/40, including the plotting routine, and will cycle completely through one time step (once through program loop) in 1 s for premelting and 1.3 s for postmelting.

Appendix B

PROGRAM LISTING

```
0001          DIMENSION TO(10,10,11,2),IXO(8,8,9),P(10,10),IH2(10,10)
             1 ,IBUF(1200),O(10)
0002    10    FORMAT(' 1 ...ALUMINUM, 2 ...COPPER, 3 ...MOLYBDENUM,')
0003    20    FORMAT(' 4 ...IRON, 5 ...NICKEL, 6 ...TITANIUM, 7 ...AL(2024)')
0004    30    FORMAT(' INPUT # FOR TARGET MATERIAL')
0005    40    FORMAT(I4)
0006    50    FORMAT(' MATERIAL THICKNESS (CM)')
0007    60    FORMAT(F20.5)
0008    70    FORMAT(' TARGET LENGTH (CM)')
0009    80    FORMAT(' TARGET WIDTH (CM)')
0010    90    FORMAT(' AMBIENT TEMPERATURE (C)')
0011    100   FORMAT(' INCIDENT POWER (WATTS)')
0012    110   FORMAT(' BEAM DIAMETER (CM)')
0013    120   FORMAT(' ANGLE OF INCIDENCE (DEG) FROM NORMAL')
0014    125   FORMAT(' PREMELT ABSORPTION COEFFICIENT')
0015    126   FORMAT(' POST-MELTING ABSORPTION COEFFICIENT')
0016    130   FORMAT(' TIME OF RUN (SEC)')
0017    135   FORMAT(' PRINT OUT INTERVAL (SEC)')
0018    140   FORMAT(' PRINT X-AXIS INTERCEPT WITH Y-Z PLANE,1-9')
0019    145   FORMAT(' LIQUID LAYER RETAINED (PERCENT OF THICKNESS)')
0020    150   FORMAT(' SELECT MODE #')
0021    151   FORMAT(' 0 ...FRONT SURFACE PLOT')
0022    152   FORMAT(' 1 ...REAR SURFACE PLOT')
0023    155   FORMAT(' 1 ...EDGES INSULATED,BACK SURFACE INSULATED')
0024    160   FORMAT(' 2 ...EDGES HEAT SINKED TO AMBIENT,BACK SURFACE
             1 INSULATED')
0025    165   FORMAT(' 3 ...EDGES INSULATED,BACK SURFACE HEAT SINKED TO
             1 AMBIENT')
0026    170   FORMAT(' 4 ...EDGES AND BACK SURFACE HEAT SINKED TO AMBIENT')
0027    172   FORMAT(' INCIDENT BEAM PROFILE')
0028    174   FORMAT(' 1 ...GAUSSIAN')
0029    176   FORMAT(' 2 ...TOP HAT')
0030    178   FORMAT(' 3 ...EXPERIMENTAL PROFILE')
0031    180   FORMAT(' FRONT SURFACE')
0032    182   FORMAT(1016)
0033    184   FORMAT(' ELEMENT',I4,'  INPUT WATTS/CM/CM')
0034    186   FORMAT(' BURN THROUGH HAS OCCURRED AT POSITION',I4,I4)
0035    188   FORMAT(' AND AT TIME',F10.5,' SECONDS')
0036    190   FORMAT(' TIME IN SECONDS',F10.5)
0037    191   FORMAT(' FRONT SURFACE')
0038    192   FORMAT(10F8.2)
0039    193   FORMAT(' BACK SURFACE')
0040    194   FORMAT(' X-Z SLICE AT Y=',I2)
0041    195   FORMAT(' RUN COMPLETED')
0042    197   FORMAT(F8.0,F8.3,F8.5,F8.3)
0043          TYPE 10
0044          TYPE 20
0045          TYPE 30
0046          ACCEPT 40,I11
0047          GO TO (200,210,220,230,240,241,242),I11
0048    200   A0=660.
0049          F0=.222
0050          F2=.497
0051          A3=2.7
0052          A4=94.
0053          F1=7.71E-5
0054          F3=9.0E-4
```

```
0055          F4=0.
0056          F5=30.
0057          F9=2.43
0058          GO TO 300
0059   210    A0=1083.
0060          F0=.915
0061          F2=.918
0062          A3=8.89
0063          A4=42.
0064          F1=2.4E-5
0065          F3=-1.19E-4
0066          F4=0.
0067          F5=18.
0068          F9=8.217
0069          GO TO 300
0070   220    A0=2610.
0071          F0=.06162
0072          F2=.346
0073          A3=10.2
0074          A4=131.
0075          F1=2.2E-5
0076          F3=-3.46E-5
0077          F4=0.
0078          F5=10.
0079          F9=8.1
0080          GO TO 300
0081   230    A0=1535.
0082          F0=.1060
0083          F2=.108
0084          A3=7.85
0085          A4=65.
0086          F1=9.6E-5
0087          F3=-1.08E-5
0088          F4=0.
0089          F5=18.
0090          F9=6.88
0091          GO TO 300
0092   240    A0=1453.
0093          F0=.1095
0094          F2=.1425
0095          A3=8.75
0096          A4=73.
0097          F1=5.49E-5
0098          F3=-4.56E-5
0099          F4=0.
0100          F5=0.
0101          F9=7.9
0102          GO TO 300
0103   241    A0=1690.
0104          F0=.139
0105          F2=.0372
0106          A3=4.54
0107          A4=103.9
0108          F1=0.
0109          F3=-4.E-6
0110          F4=0.
0111          F5=21.
```

```
0112          F9=4.09
0113          GO TO 300
0114    242   A0=630.
0115          F0=.215
0116          F2=.334
0117          A3=2.77
0118          A4=95.6
0119          F1=7.71E-5
0120          F3=9.0E-4
0121          F4=0.
0122          F5=30.
0123          F9=2.43
0124    300   TYPE 50
0125          ACCEPT 60,A6
0126          TYPE 70
0127          ACCEPT 60,A7
0128          TYPE 80
0129          ACCEPT 60,A8
0130          TYPE 90
0131          ACCEPT 60,A9
0132          TYPE 100
0133          ACCEPT 60,B0
0134          B0=B0/4.54
0135          TYPE 110
0136          ACCEPT 60,B1
0137          TYPE 120
0138          ACCEPT 60,B2
0139          TYPE 125
0140          ACCEPT 60,A5
0141          TYPE 126
0142          ACCEPT 60,AM5
0143          TYPE 130
0144          ACCEPT 60,B3
0145          TYPE 135
0146          ACCEPT 60,D0
0147          TYPE 140
0148          ACCEPT 40,ID2
0149          C9=0.
0150          TYPE 145
0151          ACCEPT 40,IH1
0152          IH1=IH1/10.+.5
0153          TYPE 150
0154          TYPE 151
0155          TYPE 152
0156          ACCEPT 40,IPL
0157          IPL=1+10*IPL
0158          TYPE 155
0159          TYPE 160
0160          TYPE 165
0161          TYPE 170
0162          ACCEPT 40,IB5
0163          TYPE 172
0164          TYPE 174
0165          TYPE 176
0166          TYPE 178
0167          ACCEPT 40,IB6
0168          B7=A8/9.
```

```
0169          B9=B1/B7
0170          B8=A7/9.
0171          C0=B1/B8
0172          GO TO (330,320,310),IB6
0173    310   TYPE 180
0174          DO 312 I=1,10
0175          DO 311 J=1,10
0176          IBUF(J)=J-1+10*(I-1)
0177    311   CONTINUE
0178          TYPE 182,(IBUF(L),L=1,10)
0179    312   CONTINUE
0180          DO 314 I=1,10
0181          DO 314 J=1,10
0182          R0=(I-5.5)**2/B9/B9+(J-5.5)**2/C0/C0
0183          IF (R0 .GT. .25) GO TO 313
0185          K=I-1+10*(J-1)
0186          TYPE 184,K
0187          ACCEPT 60,F6
0188          P(I,J)=F6/4.54
0189          GO TO 314
0190    313   P(I,J)=0.
0191    314   CONTINUE
0192          GO TO 340
0193    320   C4=4.*B0/3.14159/B1/B1
0194          DO 322 I=1,10
0195          DO 322 J=1,10
0196          R0=(I-5.5)**2/B9/B9+(J-5.5)**2/C0/C0
0197          IF (R0 .GT. .25) GO TO 321
0199          P(I,J)=C4
0200          GO TO 322
0201    321   P(I,J)=0.
0202    322   CONTINUE
0203          GO TO 340
0204    330   DO 332 I=1,10
0205          DO 332 J=1,10
0206          R0=2.*(((I-5.5)*B7)**2+((J-5.5)*B8)**2)**.5
0207          IF(R0 .GT. B1) GO TO 331
0209          E0=-2.*R0/B1
0210          P(I,J)=4.287*B0*EXP(E0)/B1/B1
0211          GO TO 332
0212    331   P(I,J)=0.
0213    332   CONTINUE
0214    340   D1=D0
0215          C1=0.
0216          DO 344 I=1,10
0217          DO 344 J=1,10
0218          DO 344 K=1,11
0219          T0(I,J,K,1)=A9
0220          T0(I,J,K,2)=A9
0221          IF(K.GT.9)GO TO 344
0223          IF(I.GT.8.OR.J.GT.8)GO TO 344
0225          IX0(I,J,K)=0
0226    344   CONTINUE
0227          C2=.2*(F0+F1*A9)*A3/(F2+F3*(A9-F5))/(1./B8/B8+1./B7/B7
             1 +100./A6/A6)
0228          D6=C2/B7/B7
0229          C0=C2*100./A6/A6
```

```
0230          C3=C2/B8/B8
0231          C4=2.*C2*(1./B8/B8+1./B7/B7+100./A6/A6)
0232          THET=3.14159*B2/180.
0233          G3=COS(THET)*A5*A6/5.
0234          B4=C2*10000./A4/A3/B8/B8
0235          B5=C2*10000./A4/A3/B7/B7
0236          B6=C2*1000000./A4/A3/A6/A6
0237          B0=0.
0238          DO 400 J=1,10
0239          DO 400 I=1,10
0240          IH2(I,J)=1
0241          B0=P(I,J)*B7*B8*4.54+B0
0242  400     CONTINUE
0243  500     IC1=8*C1+2
0244          DO 505 K=2,IC1
0245          DO 505 J=2,9
0246          DO 505 I=2,9
0247          IF(T0(I,J,K,1).LE.A0) GO TO 505
0249          IF(IX0(I-1,J-1,K-1) .NE. 0) GO TO 505
0251          T0(I,J,K,1)=A0
0252          IX0(I-1,J-1,K-1)=1
0253          IF(C1.GT..5)GO TO 505
0255          C1=1.
0256          G3=G3*AM5/A5
0257          A5=AM5
0258  505     CONTINUE
0259          DO 510 J=1,10
0260          DO 510 I=1,10
0261          I3=IH2(I,J)+1
0262          T0(I,J,I3-1,1)=(G3*P(I,J)/(F2+F3*(T0(I,J,I3,1)-F5))+
             1 4*T0(I,J,I3,1)-T0(I,J,I3+1,1))/3.
0263  510     CONTINUE
0264          DO 525 K=2,10
0265          DO 525 J=2,9
0266          DO 525 I=2,9
0267          IF(T0(I,J,K,1).LE.A0) GO TO 522
0269          F8=F9
0270          GO TO 524
0271  522     F8=A3
0272  524     A1=(F2+F3*(T0(I,J,K,1)-F5))/F8/(F0+F1*T0(I,J,K,1))
0273          E0=A1*D6*(T0(I,J+1,K,1)+T0(I,J-1,K,1))
0274          E1=A1*C0*(T0(I,J,K+1,1)+T0(I,J,K-1,1))
0275          E2=A1*C3*(T0(I+1,J,K,1)+T0(I-1,J,K,1))
0276          T0(I,J,K,2)=E0+E1+E2+(1.-A1*C4)*T0(I,J,K,1)
0277  525     CONTINUE
0278          GO TO (530,535,540,550),IB5
0279  530     DO 532 J=1,10
0280          DO 532 I=1,10
0281          T0(I,J,11,2)=T0(I,J,10,2)
0282  532     CONTINUE
0283  540     DO 533 K=2,11
0284          DO 533 J=1,10
0285          T0(1,J,K,2)=T0(2,J,K,2)
0286          T0(10,J,K,2)=T0(9,J,K,2)
0287  533     CONTINUE
0288          DO 534 K=2,11
0289          DO 534 I=1,10
```

```
0290          T0(I,1,K,2)=T0(I,2,K,2)
0291          T0(I,10,K,2)=T0(I,9,K,2)
0292    534   CONTINUE
0293          GO TO 550
0294    535   DO 537 J=1,10
0295          DO 537 I=1,10
0296          T0(I,J,11,2)=T0(I,J,10,2)
0297    537   CONTINUE
0298    550   IF(C1.LT..5) GO TO 600
0300          DO 580 K=2,10
0301          DO 580 J=2,9
0302          DO 580 I=2,9
0303          IF(IX0(I-1,J-1,K-1).LE.0) GO TO 580
0305          C7=F2+F3*(T0(I,J,K,1)-F5)
0306          E0=T0(I-1,J,K,1)+T0(I+1,J,K,1)-2*T0(I,J,K,1)
0307          IX0(I-1,J-1,K-1)=IX0(I-1,J-1,K-1)+C7*E0*B4+.5
0308          IF(IX0(I-1,J-1,K-1).GT.0) GO TO 552
0310          IX0(I-1,J-1,K-1)=1
0311    552   IF(IX0(I-1,J-1,K-1).LE.10000) GO TO 554
0313          IX0(I-1,J-1,K-1)=-1
0314          IF(K-IH2(I,J).LT.IH1)GO TO 580
0316          IH2(I,J)=IH2(I,J)+1
0317          GO TO 580
0318    554   T0(I,J,K,2)=A0
0319    560   E0=T0(I,J-1,K,1)+T0(I,J+1,K,1)-2*T0(I,J,K,1)
0320          IX0(I-1,J-1,K-1)=IX0(I-1,J-1,K-1)+C7*E0*B5+.5
0321          IF(IX0(I-1,J-1,K-1).GT.0) GO TO 562
0323          IX0(I-1,J-1,K-1)=1
0324    562   IF(IX0(I-1,J-1,K-1).LE.10000) GO TO 564
0326          IX0(I-1,J-1,K-1)=-1
0327          IF(K-IH2(I,J).LT.IH1)GO TO 580
0329          IH2(I,J)=IH2(I,J)+1
0330          GO TO 580
0331    564   T0(I,J,K,2)=A0
0332    570   E0=T0(I,J,K-1,1)+T0(I,J,K+1,1)-2*T0(I,J,K,1)
0333          IX0(I-1,J-1,K-1)=IX0(I-1,J-1,K-1)+C7*E0*B6+.5
0334          IF(IX0(I-1,J-1,K-1).GT.0) GO TO 572
0336          IX0(I-1,J-1,K-1)=1
0337    572   IF(IX0(I-1,J-1,K-1).LE.10000) GO TO 574
0339          IF(K.EQ.10)GO TO 573
0341          IX0(I-1,J-1,K-1)=-1
0342          IF(K-IH2(I,J).LT.IH1)GO TO 580
0344          IH2(I,J)=IH2(I,J)+1
0345          GO TO 580
0346    573   TYPE 186,I,J
0347          TYPE 188,C9
0348          STOP
0349    574   T0(I,J,K,2)=A0
0350    580   CONTINUE
0351    600   C9=C9+C2
0352          IF(C9.LT.D1) GO TO 700
0354          D1=D1+D0
0355          TYPE 190,C9-C2
0356    610   TYPE 191
0357          DO 620 I=1,10
0358          DO 615 J=1,10
0359          IF(1.LT.IH2(I,J))GO TO 612
```

```
0361          O(J)=TO(I,J,1,1)
0362          GO TO 615
0363    612   O(J)=1.E+9
0364    615   CONTINUE
0365          TYPE 192,(O(L),L=1,10)
0366    620   CONTINUE
0367          TYPE 193
0368          DO 630 I=1,10
0369          TYPE 192,(TO(I,L,11,1),L=1,10)
0370    630   CONTINUE
0371          TYPE 194,ID2
0372          DO 635 I=1,10
0373          DO 631 K=2,11
0374          IF(K.LT.IH2(I,ID2))GO TO 632
0376          O(K-1)=TO(I,ID2,K,1)
0377          GO TO 631
0378    632   O(K-1)=1.E+9
0379    631   CONTINUE
0380          TYPE 192,(O(L),L=1,10)
0381    635   CONTINUE
0382          E0=-500.
0383          E2=50000.
0384          DO 640 J=1,10
0385          DO 640 I=1,10
0386          IF(TO(I,J,IPL,1).LT.E0)GO TO 636
0388          E0=TO(I,J,IPL,1)
0389    636   IF(TO(I,J,IPL,1).GT.E2)GO TO 640
0391          E2=TO(I,J,IPL,1)
0392    640   CONTINUE
0393          IF(E0-E2.GT..1)GO TO 800
0395          E1=.1
0396          GO TO 850
0397    800   IF(E0-E2.GT.1.)GO TO 801
0399          E1=1.
0400          GO TO 850
0401    801   IF(E0-E2.GT.5.)GO TO 802
0403          E1=5.
0404          GO TO 850
0405    802   IF(E0-E2.GT.10.)GO TO 803
0407          E1=10.
0408          GO TO 850
0409    803   IF(E0-E2.GT.50.)GO TO 804
0411          E1=50.
0412          GO TO 850
0413    804   IF(E0-E2.GT.100.)GO TO 805
0415          E1=100.
0416          GO TO 850
0417    805   IF(E0-E2.GT.500.)GO TO 806
0419          E1=500.
0420          GO TO 850
0421    806   IF(E0-E2.GT.1000.)GO TO 807
0423          E1=1000.
0424          GO TO 850
0425    807   E1=3000.
0426    850   SCA=125./E1
0427          CALL INIT(IBUF,1120)
0428          CALL SCAL(0.,0.,970.,1000.)
```

```
0429          CALL APNT(100.,100.,-1,-1,0)
0430          CALL VECT(500.,750.,-1,6,-1,1)
0431          CALL APNT(100.,240.,-1,-1,0)
0432          CALL VECT(0.,-140.,-1,6,-1,0)
0433          CALL VECT(500.,0.,-1,6,-1,1)
0434          DO 645 I=1,5
0435          CALL APNT(I*100.+50.,90.,-1,-6,0)
0436          CALL VECT(0.,10.,-1,6,-1,1)
0437    645   CONTINUE
0438          DO 647 I=1,5
0439          CALL APNT(I*100.+40.,I*150.+25.,-1,-6,0)
0440          CALL VECT(10.,0.,-1,6,-1,1)
0441    647   CONTINUE
0442          DO 650 I=1,6
0443          CALL APNT(90.,100.+(I-1)*25.,-1,-6,0)
0444          CALL VECT(10.,0.,-1,6,-1,1)
0445    650   CONTINUE
0446          DO 660 J=1,10
0447          CALL APNT(50.+J*50.,(T0(1,J,IPL,1)-E2)*SCA+25.+J*75.,-1,-5,-1)
0448          DO 660 L=1,9
0449          CALL VECT(50.,(T0(L+1,J,IPL,1)-T0(L,J,IPL,1))*SCA,-1.5,-1,1)
0450    660   CONTINUE
0451          DO 662 I=1,10
0452          CALL APNT(50.+I*50.,(T0(I,1,IPL,1)-E2)*SCA+100.,-1,5,-1,1)
0453          DO 662 L=1,9
0454          CALL VECT(50.,(T0(I,L+1,IPL,1)-T0(I,L,IPL,1))*SCA+75.,-1,5,-1,1)
0455    662   CONTINUE
0456          CALL APNT(20.,250.,-1,-6,0)
0457          CALL TEXT(' T*C)')
0458          CALL APNT(300.,20.,-1,-6,0)
0459          IF(IPL.LT.5)GO TO 665
0461          CALL TEXT(' REAR SURFACE CENTIMETERS')
0462          GO TO 670
0463    665   CALL TEXT(' FRONT SURFACE CENTIMETERS')
0464    670   CALL APNT(0.,725.,-1,-6,0)
0465          CALL TEXT(' 3-D TEMPERATURE PROFILE')
0466          DO 675 I=1,5
0467          CALL APNT(I*100.-15.,70.,-1,-6,0)
0468          CALL NMBR(I,2*88*(I-.5),'F7.2')
0469    675   CONTINUE
0470          DO 680 I=2,5
0471          CALL APNT((I-.5)*100.,I*150.+15.,-1,-6,0)
0472          CALL NMBR(I+5,2*87*(I-.5),'F7.2')
0473    680   CONTINUE
0474          DO 685 I=1,6
0475          CALL APNT(0.,90.+(I-1)*25.,-1,-6,0)
0476          IF(E1.GT.50.)GO TO 684
0478          CALL NMBR(I+11,(I-1)*25./SCA+E2,'F6.2')
0479          GO TO 685
0480    684   CALL NMBR(I+11,(I-1)*25./SCA+E2,'F6.0')
0481    685   CONTINUE
0482          CALL APNT(0,,700.,-1,-6,0)
0483          CALL TEXT('PREPARED BY DR S.T.HANLEY N R L')
0484          CALL APNT(0.,675.,-1,-6,0)
0485          CALL TEXT('MATERIAL')
0486          CALL APNT(141.,675.,-1,-6,0)
0487          GO TO (690,691,692,693,694,810,811),I11
```

```
0488  690   CALL TEXT('ALUMINUM')
0489        GO TO 695
0490  691   CALL TEXT('COPPER')
0491        GO TO 695
0492  692   CALL TEXT('MOLYBD.')
0493        GO TO 695
0494  693   CALL TEXT('IRON')
0495        GO TO 695
0496  694   CALL TEXT('NICKEL')
0497        GO TO 695
0498  810   CALL TEXT('TITANIUM')
0499        GO TO 695
0500  811   CALL TEXT('AL(2024)')
0501  695   CALL APNT(0.,650.,-1,-6,0)
0502        CALL TEXT('BEAM POWER:')
0503        CALL APNT(156.,650.,-1,-6,0)
0504        CALL NMBR(21,B0,'F8.0')
0505        CALL APNT(290.,650.,-1,-6,0)
0506        CALL TEXT('WATTS')
0507        CALL APNT(0.,625.,-1,-6,0)
0508        CALL TEXT('IRRADIATION TIME:')
0509        CALL APNT(223.,625.,-1,-6,0)
0510        CALL NMBR(22,C9-C2,'F8.3')
0511        CALL APNT(350.,625.,-1,-6,0)
0512        CALL TEXT('S ')
0513        CALL APNT(0.,600.,-1,-6,0)
0514        CALL TEXT('ABSORPTION COEF.')
0515        CALL APNT(238.,600.,-1,-6,0)
0516        CALL NMBR(23,A5,'F8.5')
0517        CALL APNT(0.,575.,-1,-6,0)
0518        CALL TEXT('BEAM DIAMETER:')
0519        CALL APNT(193.,575.,-1,-6,0)
0520        CALL NMBR(24,B1,'F8.3')
0521        CALL APNT(335.,575.,-1,-6,0)
0522        CALL TEXT('CM')
0523  700   IF(C9.GT.B3.OR.C9.EQ.B3) GO TO 750
0525        DO 710 K=1,11
0526        DO 710 J=1,10
0527        DO 710 I=1,10
0528        TO(I,J,K,1)=TO(I,J,K,2)
0529  710   CONTINUE
0530        GO TO 500
0531  750   TYPE 195
0532        END
```